

# Refinement Mechanism of Heat-Affected Zone Microstructures on TiO Steels

Shunsuke TANIGUCHI\* Genichi SHIGESATO

## Abstract

*Nippon Steel & Sumitomo Metal Corporation has developed TiO steels with excellent HAZ toughness and applied them to offshore structures, line pipes and so on. There are two important points. One is Ti oxides have high ability as nucleation site for IGF. The other is Mn concentration control refines transformed microstructures on austenite grain boundaries. In this paper, we report the IGF transformation mechanism of Ti oxides and the suppression mechanism on grain boundary transformation by Mn concentration control as the refinement mechanism of HAZ microstructures on TiO steels.*

## 1. Introduction

As steel plates are used in welded structures, the properties of the weld zone as well as those of the base metal are important. In particular, the heat affected zone (HAZ) is heated close to the melting point of 1673 K, causing coarse grains of austenite ( $\gamma$ ) to occur. Therefore, in the HAZ structure after cooling, there are coarse grain boundary ferrite (GBF) and ferrite side plate (FSP) transformed from  $\gamma$  grain boundaries. Similar to the grain boundary cementite and martensite-austenite constituents, coarse GBF and FSP can be points of origin of fractures and cause the HAZ toughness to deteriorate markedly. Thus, to develop new steels that have good HAZ toughness, technology for refining the coarse grain microstructures forming from the  $\gamma$  grain boundaries is important.

There are two methods for refining the HAZ microstructure. One is restraining the growth of  $\gamma$  grains by utilizing pinning particles. As  $\gamma$  grains decrease in size, the microstructures of GBF and FSP formed in the cooling process are refined. As pinning particles, in addition to the TiN particles that have been commonly used,<sup>1)</sup> particles of oxides and sulfides tens of nm in size containing Mg, Ca, etc., which do not melt even at high temperatures, are especially effective.<sup>2-5)</sup>

The other method is refining GBF and FSP by utilizing the transformation of intragranular ferrite (IGF). The IGF transformation is a ferrite ( $\alpha$ ) transformation that takes place with interfaces of nonmetallic inclusions (hereinafter simply referred to as "inclusions") dispersed in  $\gamma$  grains as the nucleation site.<sup>1)</sup> Ordinarily, GBF and FSP nucleated at  $\gamma$  grain boundaries grow and increase in size toward the  $\gamma$  grains. However, when an IGF transformation occurs, GBF and

FSP collide with IGF and stop growing. Consequently, they are refined. The development of new steels utilizing the IGF transformation began in the 1970s. Various inclusions have been studied as nucleation sites. They include, for example, TiN<sup>1)</sup>, REM(O,S)-BN<sup>6)</sup>, Ca(O,S)<sup>7)</sup>, TiN-MnS-Fe<sub>23</sub>(C,B)<sub>6</sub><sup>8)</sup>, Ti<sub>2</sub>O<sub>3</sub>-TiN-MnS<sup>9-14)</sup>, Ti<sub>2</sub>O<sub>3</sub>-MnS-BN<sup>15)</sup>, and TiN-MnS<sup>16)</sup>. In the 1990s, Nippon Steel & Sumitomo Metal Corporation successfully developed TiO steels utilizing TiO oxides as nucleation sites suitable for the IGF transformation. Having high HAZ toughness, those steels are used for offshore structures, line pipes, etc. In the 2000s, to improve the HAZ toughness of TiO steels still more, the company had established not only the technology for promoting the IGF transformation but also the technology for restraining the grain boundary transformation of GBF and FSP and refining their microstructures by increasing the amount of addition of Mn.<sup>17, 18)</sup> Concerning the development of steels for offshore structures applying those technologies, Fukunaga gives a detailed account in the article "TMCP Steel Plates for Marine Structure Having High HAZ Toughness" in this special issue.

To apply the above techniques to refine HAZ microstructures on a stable basis in the actual steel manufacturing process and further enhance their functions, it is necessary to clarify the mechanisms of refinement of HAZ microstructures. This study describes the results of our studies on the mechanism of IGF transformation with a Ti oxide as the nucleation site and the mechanism of restraint on the grain boundary transformation by an increase in the amount of Mn addition. The studies were conducted using the latest transmission electron microscopy to clarify the mechanism of refinement of the HAZ microstructure of TiO steel.

\* Researcher, Materials Characterization Research Lab., Advanced Technology Research Laboratories  
1-8 Fuso-cho, Amagasaki City, Hyogo Pref. 660-0891

## 2. Mechanism of IGF Transformation with Ti Oxide as Nucleation Site

Concerning the mechanism of IGF transformation, several factors have been proposed. They include, for example, the effect of a Mn-depleted zone around the inclusion as the nucleation site, the effect of an interfacial energy arising from the lattice matching between the inclusion and  $\gamma$ ,  $\alpha$ , and the effect of a strain energy ascribable to the difference in thermal expansion coefficient between the inclusion and  $\gamma$ . However, none of them have been verified yet.<sup>19, 20)</sup> With respect to the influence of alloying elements on the IGF transformation of TiO steel, Kojima et al. report that when the amount of Mn addition was decreased from 1.6 mass% to 0.04 mass%, the rate of IGF transformation declined from 77% to 3%. Thus, Mn is an indispensable element in the IGF transformation of TiO steel.<sup>21)</sup> Therefore, paying our special attention to the Mn-depleted zone mentioned above, we examined the Mn concentration distribution on the nanometer order using a transmission electron microscope (TEM).<sup>22, 23)</sup>

The chemical composition of the sample steel was Fe-1.6Mn-0.003S-0.004N (mass%). After vacuum melting, the steel was hot-rolled into a slab. To simulate a welding heat affected zone, the slab was first heated in a high-frequency induction furnace at 1673 °K for 1 s and then cooled in such a manner that it passed the 1073 °K–773 °K region in 300 s (see Fig. 1).

After the above heat treatment, the slab was cut and the cross-section obtained was ground and etched in nital. The cross section was then observed under a scanning electron microscope (SEM) to identify from the morphology of grains the inclusion that had served as the IGF transformation nucleation site. Next, a portion of the slab containing the inclusion was extracted by using a focused ion beam (FIB) system and formed into TEM specimens on Mo grids. The specimens were subjected to quantitative elemental analysis by energy dispersive X-ray spectroscopy (EDS) with the electron beam illumination spot controlled by means of scanning transmission electron microscopy (STEM).

Figure 2 shows a STEM bright-field image of the inclusion (a) and EDS elemental maps (b)–(f). In the interface between the inclusion and  $\alpha$ , approximately 30 nm in width, there was a region where the intensity of Fe was low. This is not due to an uneven thickness the TEM specimens but due to the gradual change in thickness of  $\alpha$  because of the inclined interface between the inclusion and  $\alpha$ . Fig. 2 (d) shows the distribution of Mn. On the outside of the interface

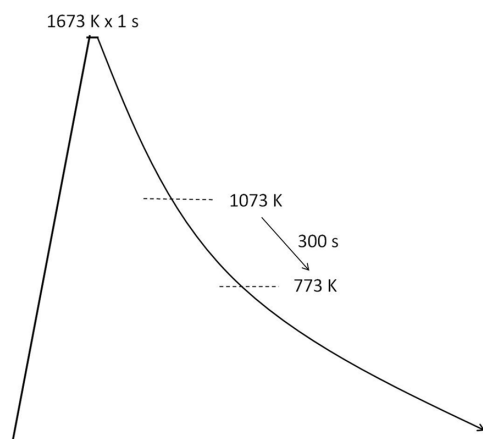


Fig. 1 Heat treatment to simulate HAZ

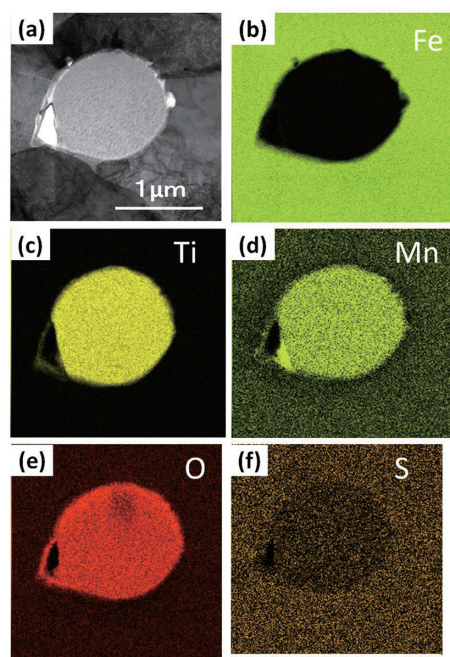


Fig. 2 STEM-EDS elemental mapping around a non-metallic inclusion of nucleation site for IGF<sup>22, 23)</sup>

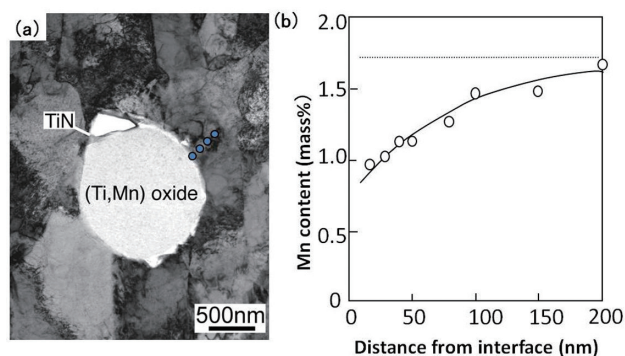


Fig. 3 Bright field TEM image of a non-metallic inclusion of nucleation site for IGF and Mn concentration profile by EDS point analysis<sup>22, 23)</sup>

overlapping region, there was a region where the Mn concentration was low. From the distributions of S, Ti, and O, it can be seen that the inclusion did not contain solute sulfur. The principal components of the inclusion were Ti and O. In addition, the inclusion contained a very small amount of solute manganese.

Figure 3 shows a bright-field TEM image of the inclusion and the Mn concentration distribution around the inclusion. The Mn concentration was quantified by an EDS point analysis on the dotted line shown in the bright-field TEM image in Fig. 3 (a). It was found that the Mn concentration decreased over a distance of about 200 nm from the inclusion and that the decrease in Mn concentration in the neighborhood of the inclusion was about 0.9 mass%.

Yamamoto, Takamura et al. suggest that the Ti oxides have cation vacancy and as Mn is absorbed into cation vacancies in Ti oxides, a large Mn-depleted zone is formed around the Ti oxides.<sup>15)</sup> It is considered that a similar phenomenon occurs with the Ti oxides in TiO steel. Mn is an element that stabilizes  $\gamma$ . It is known that when the Mn concentration decreases 1 mass%, the  $\gamma \rightarrow \alpha$  transformation point rises by about 50 K.<sup>15)</sup> The implication is that the rise in

$\gamma \rightarrow \alpha$  transformation point caused by a Mn depletion around Ti oxides promotes the IGF transformation.

### 3. Mechanism of Restraint on Grain Boundary Transformation by Increasing Amount of Addition of Mn

TiO steel utilizing the IGF transformation shows high HAZ toughness. With the aim of meeting the need for higher HAZ toughness, we developed technology for securing superior HAZ toughness on a stable basis. There were two different approaches to the technology development. One is simply increasing the amount of Ni addition. (This has long been considered effective to improve the toughness of HAZ.) The other is refining the HAZ microstructure by some means or refining the microstructures of GBF and FSP, which are the products of a grain boundary transformation. Nippon Steel & Sumitomo Metal has found that increasing the amount of addition of Mn restrains the occurrence of the grain boundary transformation.<sup>17, 18)</sup> Figure 4 compares the simulated HAZ structures of two different TiO steels having the same carbon equivalent through proper adjustment of the contents of C, Mn, Ni, and Cu.<sup>18)</sup> It is evident that the steel added with 1.92 mass% Mn, shown in Fig. 4 (a), has a finer FSP microstructure than the steel added with 1.6 mass% Mn and 0.4 mass% Cu and Ni, shown in Fig. 4 (b). We discussed the mechanism whereby GBF and FSP are refined when the content of Mn is increased. First, we made a quantitative analysis of the effect of Mn-depleted zone on the high IGF transformability that is characteristic of TiO steel. The analysis revealed that the decrease in Mn content in the neighborhood of Ti oxides was 0.7 mass%, which is almost the same as in TiO steel of the conventional chemical composition.<sup>18)</sup> Therefore, using a composition system free from the IGF transformation, we evaluated the effects of contents of Mn and Ni on grain boundary ferrite transformation. Consequently, it was found that increasing the amount of Mn addition was more effective than increasing the amount of Ni to restrain the grain boundary ferrite transformation.<sup>24)</sup> Based on the above discussions, it is considered that increasing the amount of Mn addition to TiO steel is more effective to restrain the grain boundary transformation than to promote the IGF transformation. Next, with the aim of comparing the effect of increased Mn addition on the grain boundary transformation with the effect of increased Ni addition, we studied them using model composition steels of Fe-0.3C-1X (X=Mn, Ni) mass%. As the effect on grain boundary transformation, nucleation and grain growth need to be considered separately. In the present study, as the effect on nucleation, we paid our attention to the decrease in grain boundary energy ascribable to segregation of the alloying element to the  $\gamma$  grain boundary that is the nucleation site.<sup>25)</sup>

The steel specimens used were Fe-0.31C-1.01Mn (mass%) steel

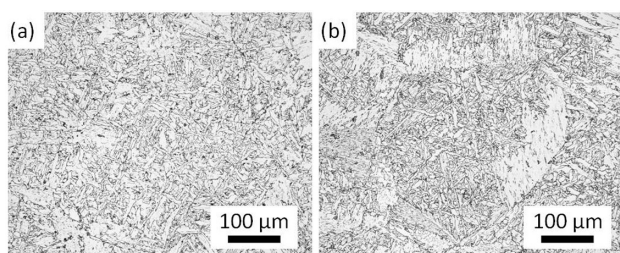


Fig. 4 HAZ microstructures of the same carbon equivalent steels with composition of a) Fe-0.06C-1.92Mn-0.001Al-0.01Ti and b) Fe-0.06C-1.60Mn-0.41Cu-0.39Ni-0.01Al-0.01Ti mass%<sup>18)</sup>

(hereinafter “1%Mn steel”) and Fe-0.31C-1.06Ni (mass%) steel (hereinafter “1%Ni steel”). After vacuum melting, each of the steel specimens was hot-rolled into a slab, which was cut into bar-shaped samples. The samples were sealed in argon gas and subjected to homogenizing treatment at 1473 K for 48 h. After that, cylindrical samples prepared from the bar-shaped ones were subjected to solution treatment at 1273 K for 30 min. The heat treatment conditions used are shown in Fig. 5. Each of the samples was first retained at 1473 K to make the  $\gamma$  grain size about 400  $\mu\text{m}$  and then kept at 1173 K for 30 min. Then, the samples whose grain boundary segregation was to be measured were subjected to water hardening. On the other hand, the samples whose nucleation behavior was to be measured were kept at 983 K for 5 to 30 s during the initial period of transformation before subjected to water quenching.

Each of the samples for examination of the nucleation behavior was cut, and the cross-section obtained was ground and subjected to nital etching. Then, the cross sections were observed under an SEM. The behavior of nucleation was evaluated in terms of the number density of ferrite particles per unit area along the prior austenite grain boundaries of the sample. At the same time, the Mn and Ni concentration distributions in the prior austenite grain boundaries were measured by using the STEM-EDS method.

With respect to the samples for measurement of grain boundary segregation, each of the cross sections was ground, and a scanning ion microscopic image thereof was observed using an FIB system. The prior austenite grain boundaries were identified from the form of crystalline grains. Then, a portion containing the identified prior austenite grain boundaries was extracted by FIB, fixed onto an Mo grid, and formed into a TEM sample, which was subjected to argon ion milling to remove the damage caused by the FIB processing. The sample was then subjected to a quantitative elemental analysis by EDS with the spot of electron beam illumination kept controlled by STEM.

Figure 6 shows an example of SEM observation of a sample for examination of nucleation. A martensitic microstructure was obtained by the water quenching. On the other hand, particles of ferrite were found along the prior austenite grain boundaries. The number of those ferrite particles was counted and divided by the observed area. The quotient obtained was used as the indicator of nucleation frequency. The frequency of nucleation was compared between 1%

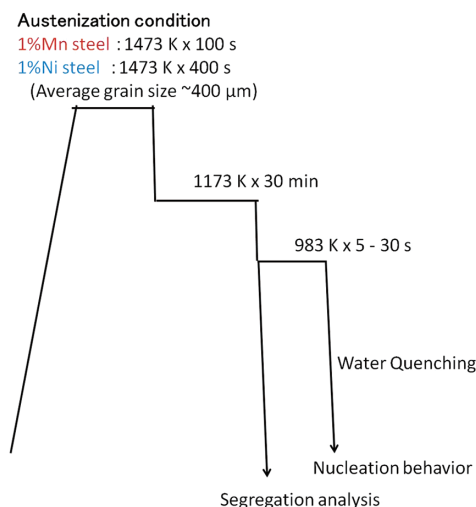


Fig. 5 Heat treatment to investigate segregation and nucleation behaviors



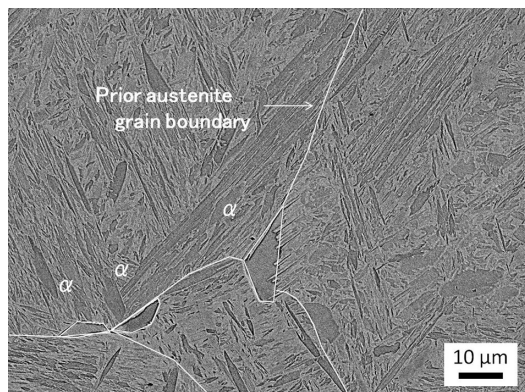


Fig. 6 Ferrite nucleation along the prior austenite grain boundaries

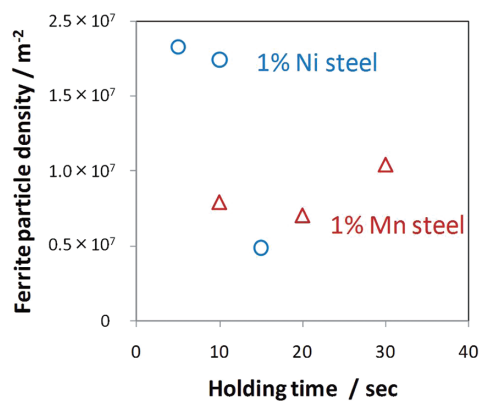


Fig. 7 Ferrite particle densities

Mn steel and 1% Ni steel. **Figure 7** shows the comparison results. The horizontal axis represents the time for which the sample was held at 983 K, and the vertical axis represents the number density of ferrite particles. On the whole, the 1% Mn steel is smaller in number density than the 1% Ni steel, suggesting that the former shows a lower frequency of nucleation.

**Figure 8** shows an example of observation of a prior austenite grain boundary using the dark-field STEM method. It can be seen that the lath structure of martensite markedly changes in direction at the prior austenite grain boundary. The samples were subjected to an EDS quantitative analysis with the spot of electron beam illumination kept changed in the direction perpendicular to the prior austenite grain boundary. **Figure 9** shows the concentration distributions of Mn and Ni in the neighborhood of the prior austenite grain boundary. At the prior austenite grain boundary, both Mn and Ni increased in concentration; however, Mn showed a larger amount of segregation. The change in grain boundary energy was calculated by using the model of Hillert et al.<sup>26)</sup> Consequently, Mn showed a larger amount of segregation and a smaller amount of decline in grain boundary energy.

From the above results, it is considered that the reason why Mn restrains the nucleation more effectively than Ni is that Mn segregates in austenite grain boundaries more than Ni, causing the austenite grain boundary energy to decrease more. In the future, it is necessary to study the effect of Mn on the growth of particles as part of the mechanism of restraint on the grain boundary transformation by an increase in amount of Mn addition.

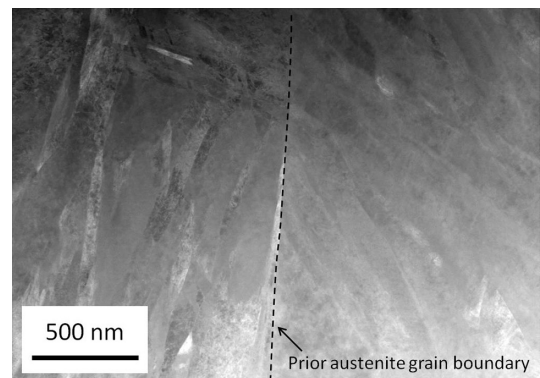


Fig. 8 STEM image of the prior austenite grain boundary

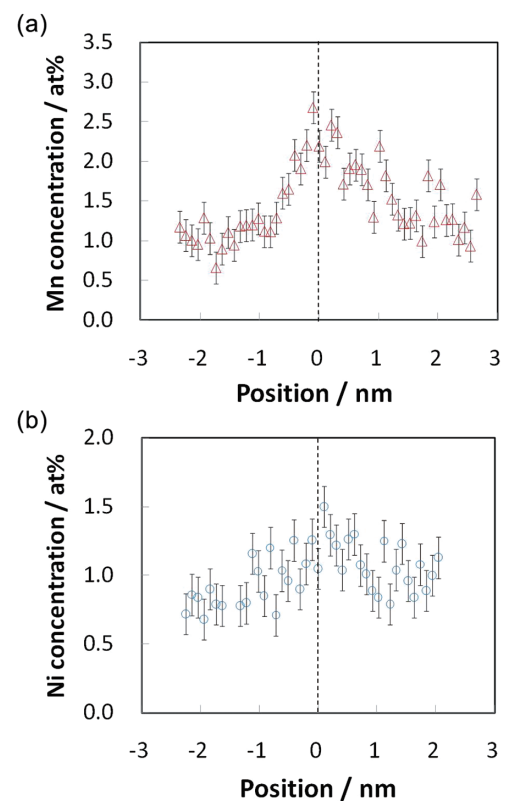


Fig. 9 Concentration profile of Mn and Ni on prior austenite grain boundary

#### 4. Conclusion

As the mechanisms of refinement of the HAZ of TiO steel, the mechanism of IGF transformation and the mechanism of restraint on the grain boundary transformation by increased addition of Mn were studied. Consequently, the following knowledge was obtained. A Mn-depleted zone is formed around Ti oxides. The rise in  $\alpha \rightarrow \gamma$  transformation point near Ti oxides caused by that Mn-depleted zone is considered to enhance the IGF transformability. In addition, the amount of Mn segregation in prior austenite grain boundaries is considerably large. The decline in prior austenite grain boundary energy caused by the segregation of Mn is considered to contribute to the restraint on nucleation.

# References

- 1) Kanazawa, S. et al.: Tetsu-to-Hagané. 61 (11), 2589 (1975)
- 2) Uemori, R. et al.: CAMP-ISIJ. 14, 1174 (2001)
- 3) Kojima, A. et al.: Welded Structure Symposium 2002, Collection of Lecture Papers. 2002, p. 327
- 4) Kojima, A. et al.: Materia. 42 (1), 67 (2003)
- 5) Kojima, A. et al.: CAMP-ISIJ. 16, 360 (2003)
- 6) Funakoshi, T. et al.: Tetsu-to-Hagané. 63, 303 (1977)
- 7) Nakanishi, M. et al.: Journal of Japan Welding Society. 52, 117 (1983)
- 8) Ohno, K. et al.: Tetsu-to-Hagané. 73, 1010 (1987)
- 9) Chijiiwa, R. et al.: Data Compiled by Welding & Metallurgical Committee. WM-1057-85, 1985
- 10) Imagunbai, M. et al.: HSLA Steels '85. 1985, p. 557
- 11) Homma, H. et al.: Welding Research Supplement. 1987, p. 301-s
- 12) Ohkita, S. et al.: Shinnittetsu Giho. (327), 9 (1987)
- 13) Chijiiwa, R. et al.: Proceedings of the 7th Int. Conf. OMAE. Houston, 1988, ASME
- 14) Yamamoto, K. et al.: Residual and Unspecified Elements in Steels. ASTM STP1042, 1988, p. 266
- 15) Yamamoto, K. et al.: Tetsu-to-Hagané. 79, 1169 (1993)
- 16) Tomita, Y. et al.: ISIJ International. 34, 829 (1994)
- 17) Terada, Y. et al.: Tetsu-to-Hagané. 90, 812 (2004)
- 18) Fukunaga, K. et al.: Proceedings of the 29th Int. Conf. OMAE. Shanghai, 2010, ASME
- 19) Shigesato, G. et al.: Tetsu-to-Hagané. 87, 93 (2001)
- 20) Iron and Steel Institute of Japan: Present Conditions of Control of Steel Microstructures and Qualities by Nonmetallic Inclusions and Study of Control Mechanisms. Tokyo, 1995
- 21) Kojima, A. et al.: CAMP-ISIJ. 16, 1530 (2003)
- 22) Sugiyama, M. et al.: Kenbikyō. 42, 69 (2007)
- 23) Shigesato, G. et al.: Ferrum, 15, 74 (2010)
- 24) Fukunaga, K. et al.: CAMP-ISIJ. 21, 620 (2008)
- 25) Taniguchi, S. et al.: Extended Abstracts of Asia Steel International Conference 2012. Beijing. 2012, CSM
- 26) Aaronson, H. I.: Lectures on the Theory of Phase Transformations. 1st ed. Metallurgical Society of AIME, 1975, p. 178



Shunsuke TANIGUCHI  
Researcher  
Materials Characterization Research Lab.  
Advanced Technology Research Laboratories  
1-8 Fuso-cho, Amagasaki City, Hyogo Pref. 660-0891



Genichi SHIGESATO  
Chief Researcher, PhD  
Plate & Shape Research Lab.  
Steel Research Laboratories